

## Yttrium-Based Porous Materials Templated by Anionic Surfactant Assemblies

Mitsunori Yada,\* Hirohumi Kitamura, Masato Machida, and Tsuyoshi Kijima

Department of Materials Science, Faculty of Engineering, Miyazaki University,  
Miyazaki, 889-2192, Japan

Received February 6, 1998

The layered and hexagonal yttrium-based surfactant mesophases templated by anionic surfactant ( $C_nH_{2n+1}OSO_3^-$  and  $C_nH_{2n+1}SO_3^-$ ) assemblies were synthesized by the homogeneous precipitation method using urea. The layered mesophase is formed of a layered but curving or bending microstructure and transformed into a hexagonal mesostructure with complex and attractive morphologies such as plate-, dish-, and crown-like shapes. The specific surface area of the mesostructured solid increases from  $53 \text{ m}^2 \text{ g}^{-1}$  for the layered form to  $251\text{--}322 \text{ m}^2 \text{ g}^{-1}$  for the hexagonal form, due to the formation of hexagonally arranged cylindrical micropores loosely occupied by surfactant molecules. The anion-exchange of the hexagonal mesophase with acetate species results in a mesoporous material with a specific surface area of as large as  $545 \text{ m}^2 \text{ g}^{-1}$ .

### Introduction

Increasing attention has been paid to a family of mesoporous materials, mostly because of their great applicabilities as catalysts, molecular sieves and host materials based on their large internal surface areas. The mesoporous materials derived by the deorganization of mesostructured inorganic/organic composites widely span from hexagonal mesoporous MCM-41<sup>1</sup> and FSM-16<sup>2</sup> silicas to titanium,<sup>3</sup> zirconium,<sup>4</sup> and other metal oxide-based analogues. Some related works concerning silica<sup>5–7</sup> or aluminum phosphate<sup>8</sup>/surfactant mesostructured systems have presented the synthesis of more attractive layered or hexagonal mesophases with complex form similar to coral, shell, diatom or other biomimetic tissues. Our recent studies reported the synthesis of aluminum- and gallium-based dodecyl sulfate mesophases with layered and hexagonal structures by the homogeneous precipitation method using urea.<sup>9,10</sup> The surfactant mesophases are of versatile morphologies such as lamellar, winding-rod, spherical, tubular, and funneled shapes depending on the urea concentration, in which the hexagonal mesophase is capable of partial transformation into an ordered mesoporous alumina under some calcination conditions.<sup>11</sup> The morphological properties of the aluminum-based mesophases as well as their crystallinities were also found to be diversely affected by anions coexisting in a reaction mixture.<sup>12</sup> The incorporation of dodecyl sulfate and alkyl alcohol in the aluminum-based mesophase leads to a layered structure with biomimetic surface patterns such as cone-

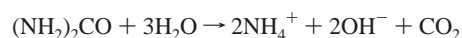
shaped or terraced hollows and domed-scales.<sup>13</sup> More recent report revealed that the anionic surfactant dodecyl sulfate is effective for the synthesis of hexagonal aluminophosphate and galloaluminophosphate mesophase which are transformed into mesoporous materials by the removal of the surfactant by anion exchange with acetate ions.<sup>14</sup>

Yttrium oxide is useful as hosts for solid-state lasers and luminescence systems, owing to its high transparency. If a mesoporous yttrium oxide is obtainable, it is thus promising not only as adsorbing or separating agents but also as a host for the homogeneous dispersion of optically functional species, followed by its postsintering.

In this paper, we report the synthesis of yttrium-based surfactant mesophases with layered and hexagonal structures and their characterization including the structural and morphological properties of both the as-grown and the deorganized solids.

### Experimental Section

The yttrium-based surfactant mesophases were synthesized by the homogeneous precipitation method using urea. Yttrium nitrate hexahydrate ( $Y(NO_3)_3 \cdot 6H_2O$ ) was used as a yttrium source and sodium dodecyl sulfate (SDS;  $CH_3(CH_2)_{11}OSO_3Na$ ) as a templating agent. Urea was used as an agent to rise the pH of solution because on heating at above  $60 \text{ }^\circ\text{C}$  it undergoes hydrolysis as follows.



Yttrium nitrate, SDS, urea, and water were mixed at a molar ratio of 1:2:30:60 and stirred at  $40 \text{ }^\circ\text{C}$  for 1 h to yield a transparent mixed solution. The mixed solution was heated at  $80 \text{ }^\circ\text{C}$  and then kept at that temperature. The pH of the reaction mixture increased from 5.2 at its initial level to 7.8 after 3 days, due to the enhanced hydrolysis of urea, while precipitation reaction occurred and developed. At a predetermined time, the resulting mixture was immediately cooled to room temperature to prevent further hydrolysis of urea. After centrifugation, the resulting solid was washed with water a few times and then dried in air. Powder X-ray diffraction (XRD) measurements were made on a Shimadzu XD-D1 diffractometer with  $Cu K\alpha$  radiation. Infrared (IR) absorption spectra were measured by the KBr pellet method using a Nippon Bunko FT/IR-300. Transmission electron microscopy (TEM) was carried out using a Hitachi H-800MU instruments. Scanning electron microscopy (SEM)

- (1) Kresge, C. T.; Leonowicz, M. E.; Roth, W. J.; Vartuli, J. C.; Beck, J. S. *Nature* **1992**, 359, 710.
- (2) Yanagisawa, T.; Shimizu, T.; Kuroda, K.; Kato, C. *Bull. Chem. Soc. Jpn.* **1990**, 63, 988.
- (3) Antonelli, D. M.; Ying, J. Y. *Angew. Chem. Int. Ed. Engl.* **1995**, 34, 2014.
- (4) Ciesla, U.; Schacht, S.; Stucky, G. D.; Unger, K. K.; Schüth, F. *Angew. Chem. Int. Ed. Engl.* **1996**, 35, 541.
- (5) Mann, S.; Ozin, G. A. *Nature* **1996**, 382, 313.
- (6) Yang, H.; Coombs, M.; Ozin, G. A. *Nature* **1997**, 386, 692.
- (7) Aksay, I. A.; Trau, M.; Manne, S.; Honma, I.; Yao, N.; Zhou, L.; Fenter, P.; Eisenberger, P. M.; Gruner, S. M. *Science* **1996**, 273, 892.
- (8) Oliver, S.; Kuperman, A.; Coombs, N.; Lough, A.; Ozin, G. A. *Nature* **1995**, 378, 47.
- (9) Yada, M.; Machida, M.; Kijima, T. *Chem. Commun.* **1996**, 769.
- (10) Yada, M.; Takenaka, H.; Machida, M.; Kijima, T. *J. Chem. Soc., Dalton Trans.* **1998**, 1547.
- (11) Yada, M.; Hiyoshi, H.; Ohe, K.; Machida, M.; Kijima, T. *Inorg. Chem.* **1997**, 36, 5565.
- (12) Yada, M.; Hiyoshi, H.; Kitamura, H.; Machida, M.; Kijima, T. *J. Porous Mater.* **1998**, 5, 133.

- (13) Yada, M.; Kitamura, H.; Machida, M.; Kijima, T. *Langmuir* **1997**, 20, 5252.
- (14) Holland, B. T.; Isbester, P. K.; Blanford, C. F.; Munson, E. J.; Stein, A. *J. Am. Chem. Soc.* **1997**, 119, 6796.

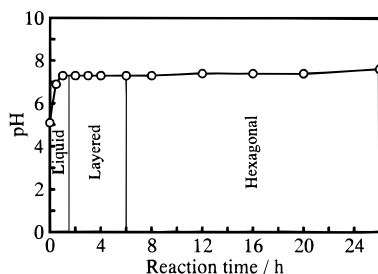


**Figure 1.** Variation of pH with time for the reaction mixture at 80 °C. The form of the products separated at different pH values is also indicated.

was performed on a Hitachi H-4100. X-ray microanalysis (XMA) was conducted by a Horiba EMAX-5770.

### Results and Discussion

The pH of the reaction mixture at 80 °C increased from 5.2 at the initial level to 7.3 after 1 h, and then remained approximately constant at 7.3–7.4 for more than 20 h until it finally reached to pH 7.8 after 78 h, as shown in Figure 1. Precipitation initiated at pH 7.3 after an induction time of 1.5 h, and the resulting white precipitates were separated at different reaction times. Figure 2A shows the XRD patterns of several selected samples. The XRD pattern of the solid separated after a 4 h reaction is characterized by three diffraction peaks at  $2\theta$

$= 1-7^\circ$ , along with a halo band at  $2\theta \sim 20^\circ$  (Figure 2A(a)). The three former peaks are attributable to the 001, 002, and 003 reflections for a layered phase with an interlayer spacing of 4.0 nm, and the halo band suggests that the short-range arrangement of constituent atoms is extremely disordered. The observed interlayer spacing can be explained by assuming that the dodecyl sulfate molecules are arranged as a bilayer between the yttrium-based inorganic layers. This crystallographic observation is consistent with the TEM image indicative of stripes based on a layered structure (Figure 3(a) and (b)) as well as the SEM image of the same sample indicating the formation of lamellar particles expected from the crystal structure (Figure 3(c)). It should be noted that the curled or fingerprint-like stripe patterns (Figure 3(a) and (b)) are arisen likely from a layered but curled or concentric layered structure, in contrast to a simple straight-extended layered structure obtained for most of Si,<sup>15</sup> Nb,<sup>16</sup> and Zr<sup>17</sup> and other metal-based layered mesophases. Such a similar curled or concentric structure was observed for chrysotile<sup>18</sup> and a layered precursor of vanadium oxide nanotube.<sup>19</sup> The maximum spacing of 4.0 nm between any two adjacent stripes is also in good agreement with the  $d_{100}$  value of 4.0 nm from X-ray diffraction, although the average value of 2.9 nm for the former is much less than the latter because most of the electromicroscopically observed lamellae are tilted relative to the incident beam. The width of the dark band

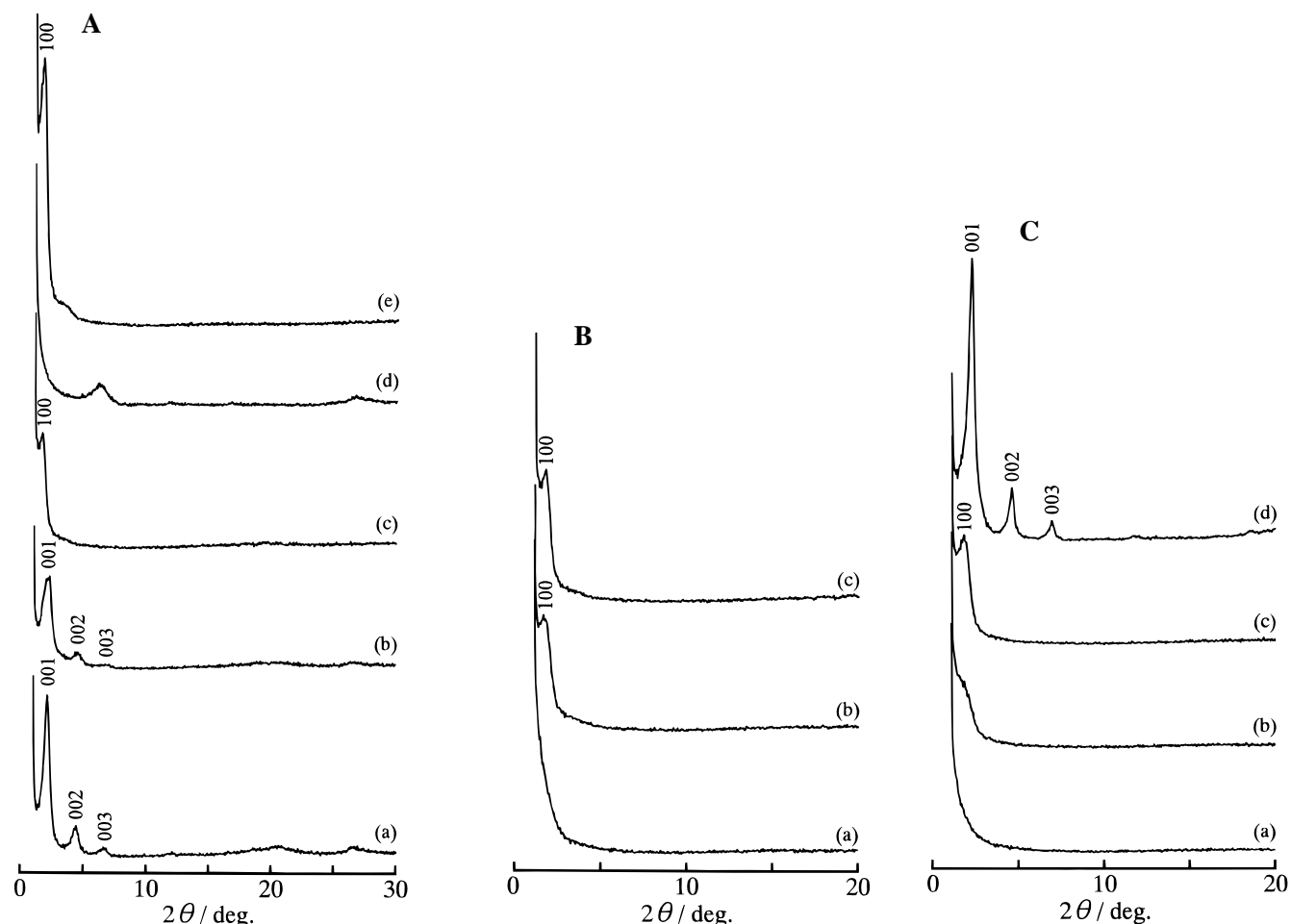
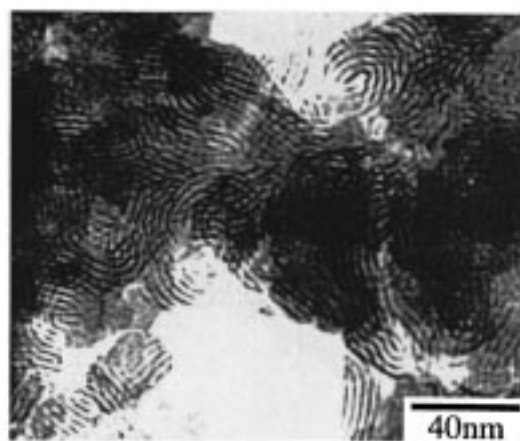
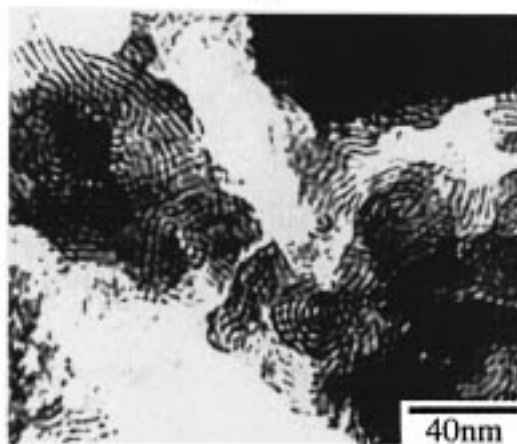


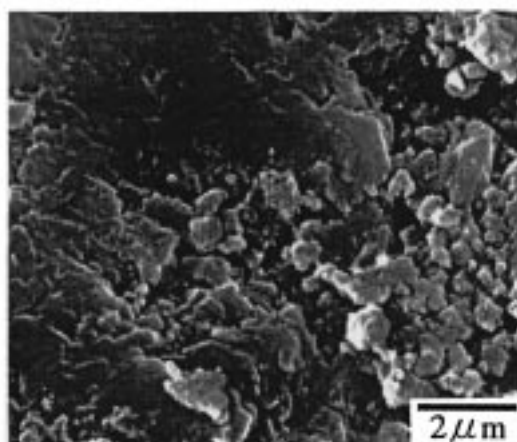
**Figure 2.** (A) Powder X-ray diffraction (XRD) patterns of as-grown samples of yttrium-based dodecyl sulfate mesophases separated at different reaction times (a–c) and the acetate-treated mesophases with layered and hexagonal structures (d–e): (a) layered phase (4 h), (b) intermediate phase (6 h), (c) hexagonal phase (20 h), (d) acetate-treated layered phase (4 h), and (e) acetate-treated hexagonal mesophase (20 h). (B) XRD patterns of as-grown samples of yttrium-based mesophase templated by sodium alkyl sulfate ( $C_nH_{2n+1}OSO_3Na$ ): (a)  $n = 8$ , (b)  $n = 10$  and (c)  $n = 12$ . (C) XRD patterns of as-grown samples of yttrium-based mesophase templated by alkyl sulfonic acid sodium salt ( $C_nH_{2n+1}SO_3Na$ ): (a)  $n = 6$ , (b)  $n = 8$ , (c)  $n = 10$ , and (d)  $n = 12$ .



a



b



c

**Figure 3.** TEM (a and b) and SEM (c) images of the yttrium-based dodecyl sulfate mesophase with a layered structure.

corresponding to the thickness of the inorganic layer is estimated to be ca. 1 nm. The dodecyl sulfate-to-Y ratio of the layered mesophase was determined by XMA to be 0.73. The above

- (15) Attard, G. S.; Glyde, J. C.; Göltner, C. G. *Nature* **1995**, *378*, 366.  
 (16) Antonelli, D. M.; Nakahira, A.; Ying, J. Y. *Inorg. Chem.* **1996**, *35*, 3126.  
 (17) Huang, Y.; Sachtler, W. M. H. *Chem. Commun.* **1997**, 1181.  
 (18) Bragg, L.; Claringbull, G. F. *The Crystalline State, Vol. 4, Crystal Structures of Minerals*; G. Bell and Sons Ltd: London, 1965; p 282.  
 (19) Spahr, M. E.; Bitterli, P.; Nesper, R.; Müller, M.; Krumeich, F.; Nissen, H. U. *Angew. Chem. Int. Ed.* **1998**, *37*, 1263.

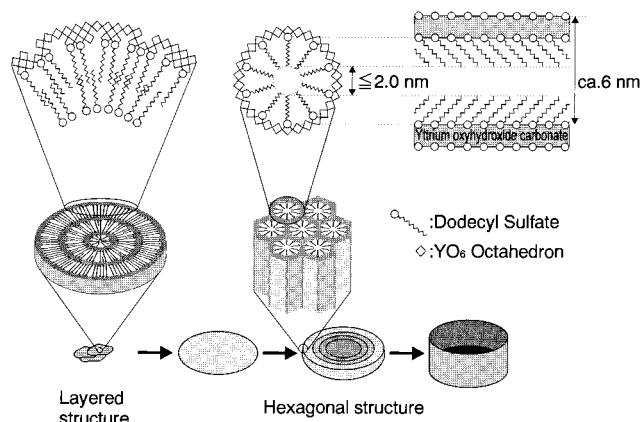


**Figure 4.** Structure models proposed for the layered and hexagonal forms and their transformation in the yttrium-based dodecyl sulfate system.

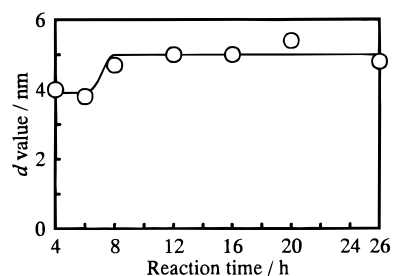


**Figure 5.** Reaction time dependence of the  $d$  value evaluated from the lowest angle reflection peak in the XRD patterns for the yttrium-based dodecyl sulfate mesostructured system.

X-ray, TEM and XMA observations suggest that the dodecyl sulfate molecules would be arranged as a bilayer between the metal oxide layers formed of two sheets of octahedral  $\text{YO}_6$  units. The curled or concentric layered structure observed above is resulted from the partial defect of  $\text{YO}_6$  octahedrons for the surfactant molecules to occupy such a specific interlayer space, as schematically represented in Figure 4.

In contrast to the layered mesophase formed at the initial stage, the mesophase obtained at longer reaction times of 8–20 h showed XRD patterns characterized by one major peak at  $2\theta = 1.6\text{--}1.8^\circ$  as well as a weak broad band at  $2\theta = 3\text{--}4^\circ$  (Figure 2A(c)). The  $d$  spacing given by the diffraction peak located at the lowest angle jumped from ca. 4.0 nm for the initially formed layered mesophase to ca. 5.0 nm for the mesophase formed at longer reaction times, as shown in Figure 5. Assuming a hexagonal cell with  $a = 6.2$  nm for the latter phase, the major peak is assignable to the 100 reflection and the broad band appears poorly resolved and located at the angles expected for the unresolved peak due to the 110 and 200 reflections. The transmission electron micrograph of the mesophase also exhibited the hexagonal array of channels, as shown in Figure 6A. Thus, the mesophases separated after an 8–20 h reaction can be taken as being a hexagonal form, though their hexagonal channels are less ordered than these in the MCM-41 silica or Al-based mesophase, as suggested from the poorly resolved 110 and 200 reflections. SEM observations revealed that the hexagonal mesophase is mainly of platelike particles clearly different in shape from the lamellar particles observed in the layered mesophase. The dodecyl sulfate-to-Y ratio of the hexagonal mesophase was determined by XMA to be 0.28, which is much less than 0.73 for the layered mesophase. The IR spectrum of the hexagonal mesophase separated after 20 h of reaction indicated two sharp peaks at  $2924$  and  $2854\text{ cm}^{-1}$  due to  $[\nu(\text{CH}_2)]$  and a peak at  $2958\text{ cm}^{-1}$  due to the  $[\nu(\text{CH}_3)]$



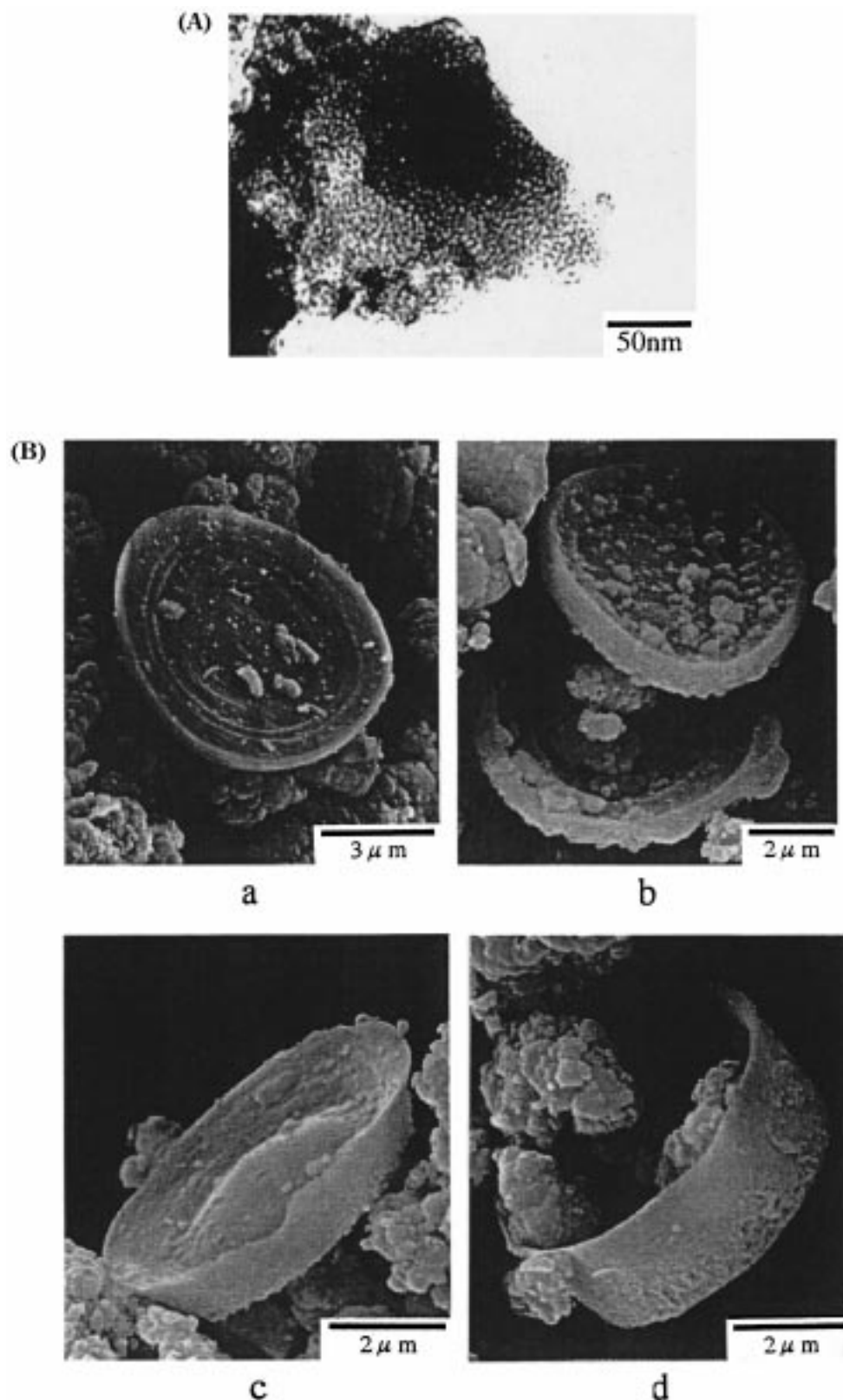


**Figure 6.** TEM (A) and SEM (B) photographs of the yttrium-based dodecyl sulfate mesophase with a hexagonal structure. (A) Hexagonal arrays viewed along the channel axis. (B) (a) Disklike particle with surface patterns of concentric circles; (b) disklike particle with a terraced hollow; (c) platelike particle; and (d) dish-like particle.

group, along with two peaks at 1248 and 1213  $\text{cm}^{-1}$  associated with R-OSO<sub>3</sub><sup>-</sup> group. Additional broad band attributable to CO<sub>3</sub><sup>2-</sup> group also appeared in the range of 1300–1700  $\text{cm}^{-1}$ . This is consistent with a previous report that spherical particles of yttrium basic carbonate, Y(OH)CO<sub>3</sub>, are formed from a SDS-free yttrium solution by the homogeneous precipitation method

using urea.<sup>20</sup> It is thus reasonable to assume that the hexagonal mesophase is composed of yttrium oxyhydroxide, carbonate and dodecyl sulfate species. The solid separated at pH 7.4 after 6 h of reaction (Figure 2A(b)) gave broad 001, 002, and 003 peaks, being suggestive of a layered structure with a lower crystallinity than the solid separated after 4 h of reaction. Therefore, this

solid is likely an intermediate phase between the layered and hexagonal mesophases, if the specific surface area described later is also taken into consideration. The solid separated at pH 7.8 after 76 h was a hexagonal mesophase with a low crystallinity, as suggested from the marked decrease of the 100 reflection as well as the formation of indefinite-shaped particle.

The above XRD, SEM, and TEM observations as a function of reaction time or pH suggest that the layered mesophase initially precipitated is structurally converted into a more stable hexagonal form, as in the aluminum-based dodecyl sulfate system.<sup>11</sup> Urea is essential for the layer to hexagonal transition, because the reaction using aqueous ammonium solution in place of urea yields only a layered mesophase with an interlayer spacing of 4.0 nm, as observed in the aluminum-based system.<sup>11</sup> This is probably due to the gradual and homogeneous supply of hydroxide ions and the stabilization of surfactant assemblies by urea. In keeping with this indication, the layered mesostructured particles were morphologically transformed mostly from lamellar into platy but bulky form, as shown in Figure 6B(a) and (b). The layer to hexagonal transition would occur through the partial condensation and cross-linking of yttrium oxyhydroxide layers interleaved with dodecyl sulfate bilayers, accompanied by the rearrangement of the bilayered surfactant molecules into a rodlike assembly, as observed in FSM-16<sup>2</sup> and aluminum-based mesostructured systems.<sup>11</sup> Additional SEM images of the yttrium-based hexagonal mesophase separated at 20 h further indicated partial formation of morphologically unique particles, as shown in Figure 6B(c) and (d). The particle shown in Figure 6B(a) is of disklike form with a surface pattern of concentric circles. The particles observed in Figure 6B(b) and (c) are of platelike form with a terraced hollow, and the particle shown in Figure 6B(d) is of dish or crown-like form. The above SEM observations comprehensively suggest that the hexagonal mesostructured crystals occur frequently in the form of disklike particles, and some of them further develop predominately at the external edges into crown-like ones, as schematically proposed in Figure 4. Such unique morphologies would be originated from the precursory lamellar particles having a bending, winding, concentric, or fingerprint-like structure, as shown in Figure 3(a) and (b).

Similar reactions using sodium alkyl sulfate ( $C_nH_{2n+1}OSO_3Na$ ,  $n = 8-10$ ) in place of SDS were done using a reaction time of 20 h, and the XRD patterns of the obtained solids are shown in Figure 2B. Although the  $n = 10$  product gave a hexagonal mesophase with a  $d_{100}$  value of 5.0 nm equal to that of the  $n = 12$  product, the  $n = 8$  product gave neither diffraction peak in the XRD pattern nor signals attributable to the surfactant in the IR and XMA spectra. The S-to-Y molar ratio for the  $n = 10$  product was determined to be 0.18, a little less than 0.28 for the yttrium-based dodecyl sulfate mesophase separated at 20 h. The use of sodium salts of  $n$ -alkyl sulfonic acid ( $C_nH_{2n+1}SO_3Na$ ;  $n = 8-12$ ) in place of SDS also resulted in the formation of yttrium-based surfactant mesophases. The XRD patterns of the resulting solids are shown in Figure 2C. Although neither XRD peak nor surfactant-associated IR or XMA signal is observed for the  $n = 6$  product, the XRD pattern of the  $n = 8$  product gives a shoulder peak near  $2\theta = 1.5-2.0^\circ$ , and the pattern of the  $n = 10$  product is suggestive of a hexagonal structure, similarly to that for the SDS templating system. The S-to-Y molar ratio for the  $n = 10$  product was determined to be 0.24, in good agreement with 0.28 for the yttrium-based dodecyl sulfate mesophase separated at 20 h. The appearance

of the hexagonal mesophase for the  $n = 10$  product in either the alkyl sulfonate or alkyl sulfate system is resulted from the formation of stable rodlike surfactant assemblies to aggregate together with yttrium species, due to the enhanced van der Waals interaction between the long chain surfactant molecules. It should be noted that the  $n = 10$  products in both the alkyl sulfonate and sulfate systems give nearly the same  $d_{100}$  value of 5.0 nm as that for the hexagonal mesophase templated by dodecyl sulfate assemblies, and that even the  $n = 8$  product in the alkyl sulfonate system yields a shoulder peak at the same angle as the  $n = 10$  product. This is strikingly different from the fact that the cell parameter  $a$  for the mesoporous silica<sup>1</sup> and the aluminum-based surfactant mesophases<sup>11</sup> shows a tendency to increase with an increase of the carbon number of the surfactant used. These data indicate that the unit cell parameter  $a$  of the yttrium-based hexagonal mesophase is little dependent on the length of surfactant molecule and essentially determined by the dimension of framework of yttrium-oxyhydroxide-carbonate clusters including surfactant assemblies. The hexagonal structure could occur even at low loadings of surfactants with a moderate chain length from a layered structure. On the other hand, the XRD pattern of the  $n = 12$  product is indicative of a layered structure, similarly to the yttrium-based dodecyl sulfate mesophase separated at 4 h. The S-to-Y molar ratio determined by XMA was 1.05, in close agreement with 0.73 for the layered yttrium-based dodecyl sulfate mesophase separated at 4 h. This is because the layered structure formed in the initial stage of precipitation is so stable as to hamper the layer to hexagonal transition. The longer alkyl chain, the more stable the layered structure is retained by the van der Waals attraction between alkyl chains of surfactants. The structural difference between the two  $n = 12$  products templated by dodecyl sulfonate and dodecyl sulfate would be attributable to the difference in bulkiness between the sulfonate and sulfate headgroups in both surfactants. When sodium laurate ( $CH_3(CH_2)_{10}COONa$ ) and dodecyl phosphoric acid ( $C_{12}H_{25}OPO(OH)_2$ ) were used in place of SDS, a white solid precipitated almost instantly and inhomogeneously on addition of the anionic surfactant.

Since the as-grown hexagonal mesophases collapsed into amorphous solid on calcination at 300 °C, an attempt was made to remove the surfactant species from the mesophase by anion exchange with acetate anions. The layered or hexagonal mesophase sample (0.5 g) was mixed with 0.05 M ethanol solution of sodium acetate (40 mL), and then allowed to stand under stirring at 40 °C for 1 h. The resulting solids were fully washed with ethanol and dried in air. As a result of the acetate treatment, the layered phase greatly decreased in interlayer spacing from 4.0 to 1.4 nm with an accompanying decrease in crystallinity, as suggested from the single XRD peak at  $2\theta = 6.2^\circ$  for the curve d in Figure 2A. The  $d$  spacing of 1.4 nm is close to 1.0 nm for the thickness of inorganic layer estimated from the TEM image of the as-grown sample. This fact suggests that most of the incorporated dodecyl sulfate species was exchanged with acetate ions, in keeping with the XMA observation indicating a remarkable decrease of the S-to-Y ratio from 0.73 to 0.23. On the other hand, the hexagonal mesophase showed a tendency to convert into a more developed hexagonal structure with a unit cell parameter of  $a = 6.1$  nm by the acetate-treatment, as suggested from its XRD pattern indicative of the intensified 100 peak as well as a broad but more definite band at  $2\theta = 3-4^\circ$  deconvoluted into the 110 and 200 reflections (Figure 2e). Little sulfur species were detectable by the XMA analysis for the acetate-treated sample. This was also confirmed by the IR spectrum of the same sample which shows no

(20) Aiken, B.; Hsu, W. P.; Matijevic, E. *J. Am. Ceram. Soc.* **1988**, *71*, 845.

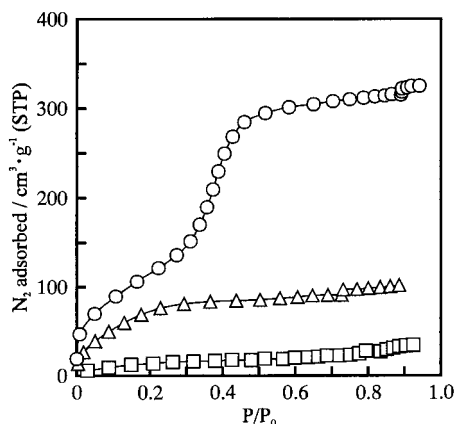


**Figure 7.**  $N_2$  adsorption isotherms of the yttrium-based dodecyl sulfate mesophases: ( $\square$ ) layered (as grown), ( $\Delta$ ) hexagonal (as grown), and ( $\circ$ ) hexagonal (acetate-treated).

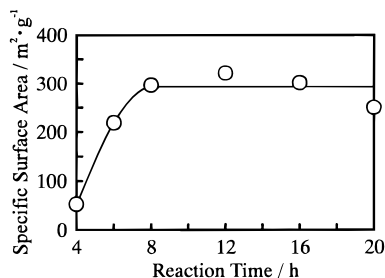


**Figure 8.** Plots of the specific surface areas of the yttrium-based dodecyl sulfate mesophases against the reaction time.

absorption peaks attributable to dodecyl sulfate. These IR and XMA data suggest the complete removal of dodecyl sulfate species. When the hexagonal mesophase was treated with ethanol alone, no dodecyl sulfate species were released from the mesophase. Thus the acetate-treatment is effective for the complete removal of the incorporated dodecyl sulfate anions in the yttrium-based mesophase while keeping the hexagonal structure, as demonstrated for the aluminophosphate and galloaluminophosphate systems.<sup>14</sup>

The porous properties of all the yttrium-based mesophases obtained were characterized based on their  $N_2$  adsorption behavior. Prior to the adsorption measurement, samples were heated at 150 °C for 1 h in a vacuum to remove adsorbed water. The  $N_2$  adsorption isotherms for as grown samples of the typical layered and hexagonal mesophases are shown in Figure 7. Both curves exhibit one-step adsorption of  $N_2$ , and the  $N_2$  amount adsorbed for the hexagonal form is about four times larger than that for the other over the entire range of  $P/P_0$ . This was confirmed more definitely by a remarkable increase of the specific surface area of the mesostructured solids from 53  $m^2 g^{-1}$  for the layered form to 251–322  $m^2 g^{-1}$  for the hexagonal form (Figure 8). The pore size distribution determined by Clanston–Inkley method<sup>21</sup> indicated a shoulder peak below 2.0 nm shown in Figure 9. The observed decrease of the S-to-Y molar ratio from 0.73 to 0.28 due to the layer to hexagonal transition is also because a considerable amount of surfactant molecules were desorbed so as to compensate the decreased positive charge of the inorganic framework due to the condensation of yttrium oxyhydroxide species. It is thus suggested that the remaining surfactant molecules bound to the inorganic wall would be arranged as a loosely packed monolayer with their chains tilted relative to the wall to form a micropore in the

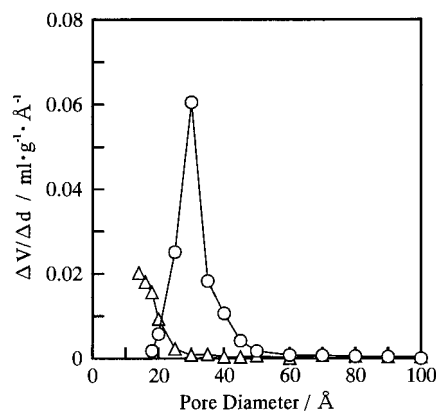


**Figure 9.** Pore size distributions of the hexagonal yttrium-based dodecyl sulfate mesophases: ( $\Delta$ ) as grown, ( $\circ$ ) acetate-treated.

cylindrical space, as schematically shown in Figure 4. Here the inorganic wall is so thick and rigid that the hexagonal framework would be stably formed only with a few degrees of mechanical support by the surfactant assemblies, though the surfactant molecules would act as a templating agent to induce the layer to hexagonal transition. The proposed structure model is also consistent with the X-ray observations that the unit cell parameter  $a$  of the yttrium-based hexagonal mesophase is independent of the chain length of the surfactant used.

More interestingly, the porous character of the hexagonal mesophase was drastically improved by the acetate treatment, as suggested from the  $N_2$  adsorption isotherm for the resulting solid in Figure 7. The  $N_2$  adsorption curve shows two distinct partial-pressure regions. The  $N_2$  adsorption at  $P/P_0 = 0-0.3$  is due to the monolayer coverage of mesopores and particle surface, whereas that at  $P/P_0 = 0.3-0.5$  is characteristic of capillary condensation in mesopores. The specific surface area of this mesoporous composite was as large as 545  $m^2 g^{-1}$  being about two times larger than that for the as-grown hexagonal phase and the effective pore size was determined to be 3.0 nm, as shown in Figure 9. Taking into consideration the  $YO_{1.5}$  to  $SiO_2$  mass ratio of 113/60, the present mesoporous yttrium oxide corresponds to a mesoporous silica with a specific surface area of 1026  $m^2 g^{-1}$ , equivalent to that ( $= 1000 m^2 g^{-1}$ ) observed for MCM-41<sup>1</sup> or FSM-16.<sup>2</sup> On calcination at 800 °C for 10 h, the acetate-treated mesoporous material completely collapsed and converted into yttrium oxide ( $Y_2O_3$ ) with a specific surface of as small as 18  $m^2 g^{-1}$ . A similar observation was made for the as-grown hexagonal phase to yield a mixture of yttrium oxide and yttrium oxide sulfate ( $Y_2O_2SO_4$ ) with a specific surface of 17  $m^2 g^{-1}$ . The yttrium-based hexagonal mesoporous materials are thus promising as an adsorbent or separating agent as well as a host matrix for optical or other functional species, although they are not suitable for high-temperature processes or applications.

In conclusion, we report the synthesis of layered and hexagonal mesostructured yttrium oxides templated by anionic surfactant assemblies using the homogeneous precipitation method using urea. The yttrium-based surfactant mesophases with lamellar, dishlike, or other complex morphologies and surface patterns might be useful for clarifying the pathway of biomineralization in coral, shell, diatom or other calcified tissues. The yttrium-based micro- or mesoporous materials would contribute to the development of functional mesostructured materials such as host matrixes, optical materials or precursors of high-temperature ceramics.

(21) Cranston, R. W.; Inkley, F. A. *Adv. Catal.* **1957**, *9*, 143.